

Human VRK2 modulates apoptosis by interaction with Bcl-xL and regulation of *BAX* gene expression

DM Monsalve^{1,2}, T Merced¹, IF Fernández^{1,2}, S Blanco^{1,3}, M Vázquez-Cedeira^{1,2} and PA Lazo^{*1,2}

VRK2 is a novel Ser-Thr kinase whose VRK2A isoform is located in the endoplasmic reticulum and mitochondrial membranes. We have studied the potential role that VRK2A has in the regulation of mitochondrial-mediated apoptosis. VRK2A can regulate the intrinsic apoptotic pathway in two different ways. The VRK2A protein directly interacts with Bcl-xL, but not with Bcl-2, Bax, Bad, PUMA or Bnip-3L. VRK2A does not compete with Bax for interaction with Bcl-xL, and these proteins can form a complex that reduces apoptosis. Thus, high VRK2 levels confer protection against apoptosis. In addition, VRK2 knockdown results in an increased expression of *BAX* gene expression that is mediated by its proximal promoter, thus VRK2A behaves as a negative regulator of *BAX*. Low levels of VRK2A causes an increase in mitochondrial Bax protein level, leading to an increase in the release of cytochrome C and caspase activation, detected by PARP processing. VRK2A loss results in an increase in cell death that can be detected by an increase in annexinV+ cells. Low levels of VRK2A increase cell sensitivity to induction of apoptosis by chemotherapeutic drugs like camptothecin or doxorubicin. We conclude that VRK2A protein is a novel modulator of apoptosis. *Cell Death and Disease* (2013) 4, e513; doi:10.1038/cddis.2013.40; published online 28 February 2013

Subject Category: Experimental Medicine

The intrinsic apoptotic pathway is partly controlled by proteins present on the mitochondrial membrane. This apoptotic protein family is defined by the structural characteristics of its BH (Bcl-2 homology) domains.¹ There are four types of BH domains and their combination determine the interaction of these proteins;^{2–4} some are anti-apoptotic, such as Bcl-2 and Bcl-xL, or pro-apoptotic, such as Bax.^{2,3,5,6} Others only have a unique BH3 domain and are subdivided in activators of proapoptotic proteins, such as Bid, or inhibitors of anti-apoptotic proteins, such as PUMA α , Bad or Bnip3L. These proteins also have a transmembrane domain in their C-terminal region. The activation of the apoptotic signal activates the translocation of cytosolic Bax to the outer mitochondrial membrane and induces the release of cytochrome c.⁷

Apoptosis is further controlled by the interaction of these BH proteins with other cellular proteins. In Epstein–Barr virus-infected cells, the BHRF1 protein, a viral homologue of mammalian Bcl-2, has a protective role against apoptosis.⁸ This protective role detected in infected cells is mediated by the direct interaction between viral BHRF1 and cellular VRK2A.^{8,9} Thus, apoptosis is also modulated by additional cellular proteins which in general are not known. Based on this observation, we hypothesized that VRK2A might have a

protective role against apoptosis if it could interact with, and regulate, proteins that participate in the mechanisms that trigger or execute apoptosis in human cells.

The VRK (vaccinia-related kinase) family of protein kinases forms a divergent branch in the human kinome,¹⁰ composed of three members,¹¹ but only two of them, VRK1¹² and VRK2¹³ are catalytically active kinases. These proteins present sequence and structural differences in their kinase domain with respect to most kinases, and have an unrelated C-terminal region.^{13,14} Their activity can be regulated by protein–protein interactions, such as interaction with the small GTPase Ran¹⁵ or histones.¹⁶ VRK1 is a nuclear protein implicated in cell cycle regulation¹⁷ that behaves like an early gene,^{18,19} and also participates in additional processes such as DNA-damage responses,²⁰ Golgi fragmentation,²¹ nuclear envelope dynamics⁹ and chromatin condensation.¹⁷ Among its phosphorylation targets are transcription factors such as p53,¹² c-Jun,²² ATF2²³ and CREB.¹⁹

The VRK2 protein has two isoforms generated by alternative splicing.²⁴ One of them, VRK2A, also known as VRK2,¹³ is the canonical full-length protein and has 508 amino acids with a C-terminus transmembrane domain.^{13,24} VRK2A is anchored to the endoplasmic reticulum and mitochondria.²⁴ VRK2B is a shorter isoform that has 397

¹Experimental Therapeutics and Translational Oncology Program, Instituto de Biología Molecular y Celular del Cáncer, Centro de Investigación del Cáncer, CSIC—Universidad de Salamanca, Campus Miguel de Unamuno, Salamanca, Spain; ²Instituto de Investigación Biomédica de Salamanca (IBSAL), Hospital Universitario de Salamanca, Salamanca, Spain and ³Wellcome Trust-Medical Research Council, Cambridge Stem Cell Institute, University of Cambridge, Cambridge, England

*Corresponding author: P A Lazo, Experimental Therapeutics and Translational Oncology Program, Instituto de Biología Molecular y Celular del Cáncer, Centro de Investigación del Cáncer, CSIC—Universidad de Salamanca, Campus Miguel de Unamuno, Salamanca E-37007 Spain. Tel: +34 923 294 804; Fax: +34 923 294 795; E-mail: pedro.lazo@csic.es

The protein interactions from this publication have been submitted to the European Bioinformatics Institute-EMBL IMEx (<http://www.imexconsortium.org/>) consortium through IntAct (pmid 19850723) and assigned the identifier IM-18530.

Keywords: VRK2; Bcl-xL; apoptosis; protein–protein interactions; chemotherapy

Abbreviations: VRK, vaccinia-related kinase; MAPK, mitogen-activated protein kinase; JIP, c-Jun N-terminal kinase interacting protein; KSR, kinase suppressor of Ras
Received 26.9.12; revised 15.12.12; accepted 28.1.13; Edited by G Ciliberto

amino acids, lacks the transmembrane region and is detected free in nucleus and cytosol.²⁴ Both isoforms have, *in vitro*, a similar pattern of phosphorylation substrates²⁵ and sensitivity to kinase inhibitors.^{24,26} Thus, the specificity of their biological effects is most likely determined by their subcellular localization and the proteins present in their local microenvironment. VRK2A anchored to the endoplasmic reticulum is able to modulate cellular responses mediated by MAPK signalling pathways.^{27–30} VRK2A directly interacts with the JIP1 scaffold protein, forming signalosomes with a very high molecular size, > 1000 kDa.^{27,28} The inclusion of VRK2A in these complexes prevents the phosphorylation of c-Jun in response to hypoxia²⁷ or interleukin-1 β .²⁸ Mechanistically, the interaction between VRK2A and JIP1 prevents the incorporation of JNK (c-Jun N-terminal kinase) to the complex, thus c-Jun cannot be phosphorylated. Reduction in VRK2A levels results in an increased response mediated by this pathway.^{27,28} Moreover, VRK2 can form a macromolecular complex by interacting with the KSR1 scaffold protein and this interaction reduces signalling mediated by MAPK in response to ErbB2 in breast cancer,^{29,30} and to activated oncogenes such as Ras and B-Raf²⁹ mutants. A subpopulation of VRK2A was also identified located on the mitochondrial membrane,²⁴ but no function is known to be associated to its presence on this organelle. Therefore, we tested whether this VRK2A subpopulation was able to affect the intrinsic apoptotic pathway,³¹ which is mediated by mitochondria.³¹ In this study, it has been identified that VRK2A levels can modulate apoptosis in two different ways, by its interaction with Bcl-xL and by regulation of *BAX* gene expression.

Results

VRK2A colocalized with Bcl-xL, Bcl-2 and Bax, but only interacted with Bcl-xL. The subcellular localization of proteins can determine their role in specific biological functions. Although most of the VRK2 isoform A (full-length protein) is anchored to the endoplasmic reticulum membrane, a minor VRK2A subpopulation is located in the mitochondria,²⁴ suggesting that this VRK2A subpopulation might participate in the regulation of cellular functions mediated by mitochondria, as is the case with the intrinsic apoptotic pathway.⁷ Based on the interaction between VRK2A and the Epstein–Barr virus BHRF1 protein, a viral homologue of anti-apoptotic Bcl-2 that interacts with Bcl-2,⁸ it is a possibility that VRK2A might also have effects probably mediated by an interaction between VRK2A and apoptotic proteins of the Bcl-2 family, of which, Bcl-xL is the antiapoptotic protein expressed in most cell types. Initially, it was tested if VRK2A could colocalize with any of the proteins that participate in apoptosis. Endogenous VRK2A showed an overlapping confocal immunofluorescence signal with Bcl-xL (Figure 1a), and with the proapoptotic Bax (Figure 1b), suggesting that they are physically proximal, but this does not mean that they are directly interacting.

Next, it was determined if there was a direct association between these proteins. For this aim, cells were transfected with GST-VRK2A, and the associated endogenous proteins were brought down in pulldown assays and identified in immunoblots. Only endogenous Bcl-xL, but not Bcl-2 or Bax,

interacted with VRK2A (Figure 1c). The interaction region was mapped to the C-terminus of VRK2A between residues 397–508, located between the kinase domain and the membrane anchor region (Figure 1d), according with the VRK2 region interacting with Epstein–Barr BHRF1 protein.⁸ Moreover, an additional, and weaker, interacting region was identified, which was also detected between residues 1–320 of VRK2A (Figure 1d), but this region containing part of the kinase domain is not correctly folded.¹⁴ The interaction with Bcl-xL was also detected with kinase-dead VRK2 (K179E) protein (not shown), and thus it was independent of VRK2 kinase activity.

The potential interaction of VRK2A with BH3-only proteins, such as PUMA α , BAD and Binp3L was ruled out using a similar approach (Supplementary Figure S1).

Bax did not directly interact with VRK2A, but it was present in VRK2A–Bcl-xL complexes.

One possible consequence of the interaction between VRK2A and Bcl-xL is that it might interfere with the formation of the Bcl-xL–Bax complex. To determine the effect on the different interactions, each of the components was varied in the presence of saturating amounts of the other proteins. When Bax was increased, the amount of Bax detected in the GST-VRK2A pulldown increased accordingly (Figure 2a). These data indicated that a fraction of the VRK2A–Bcl-xL complex was able to incorporate Bax. Moreover, increasing amounts of Bcl-xL resulted in an increase in its presence in the GST-VRK2A pulldown (Figure 2b), indicating that Bcl-xL was necessary to form this three-protein complex, and was the likely bridge between the other two proteins. Bax was always present in the complex and did not increase, suggesting that its interaction was not facilitated by the presence of VRK2A, and indicating that the maximum effect was already reached (Figure 2a). When saturating amounts of Bcl-xL and Bax were used, and VRK2 was increased, there was more VRK2A bound to the complex at the higher concentrations, suggesting that saturation was already reached (Figure 2c), and that a ternary complex was being formed. From these data, it could be concluded that VRK2A forms a complex with these two proteins without competition for their interaction.

To determine if VRK2A was able to phosphorylate either Bcl-xL or Bax, different *in vitro* kinase assays were performed. VRK2A did not phosphorylate any of these proteins (not shown).

VRK2 regulated the expression of BAX gene. One mechanism by which VRK2 might regulate apoptosis is by regulating, directly or indirectly, the expression of *BAX*, which is essential for triggering apoptosis. Therefore, it was first tested if the level of Bax protein was affected by the knockdown of VRK2. VRK2 knockdown resulted in an increase in Bax protein levels, both total protein recognized by antibody 2D2, and activated Bax recognized by antibody 6A7 (Figure 3a), suggesting that VRK2A protein had a negative effect on Bax expression or stability. Furthermore, a reduction in the levels of anti-apoptotic proteins Bcl-2 and Bcl-xL was detected when VRK2 was knocked down, suggesting a role of VRK2 in protecting cells from apoptosis.

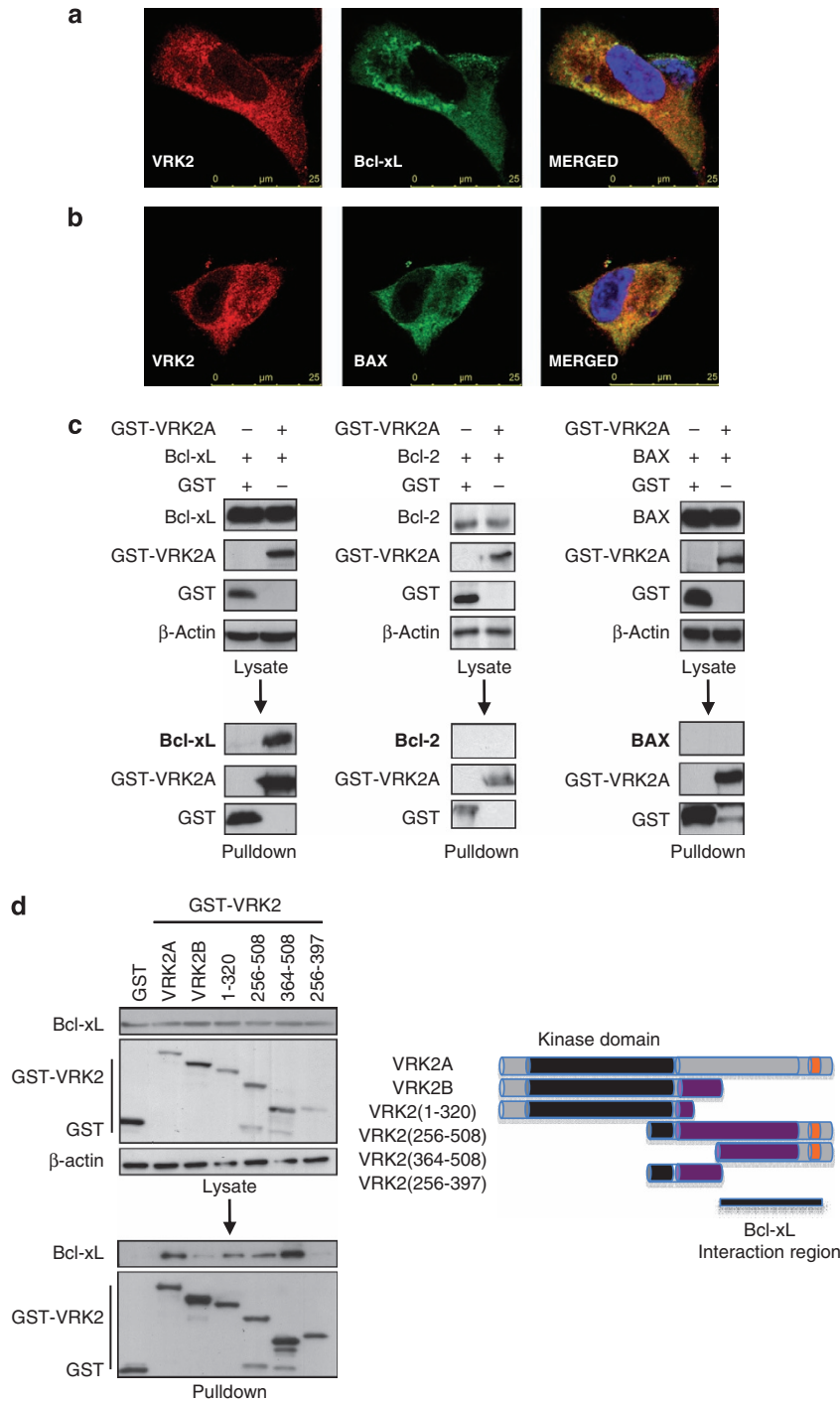


Figure 1 Subcellular localization and interactions of VRK2A with apoptotic proteins. **(a)** Colocalization of endogenous VRK2 with transfected Bcl-xL detected by confocal microscopy in A549 cells. VRK2 was detected with a rabbit polyclonal antibody and Bcl-xL with a monoclonal antibody. **(b)** Colocalization of VRK2 with transfected Bax detected by confocal microscopy in A549 cells. Bax was detected with a monoclonal antibody. **(c)** Detection of interaction between VRK2 and Bcl-xL, Bcl-2 or Bax in pull-down assays. HeLa cells were transfected with plasmid pCEFL-GST-VRK2A that expresses GST-VRK2A and used in a pull-down assay in which the associated protein were detected in immunoblots using specific antibodies for GST that detects transfected GST and GST-VRK2A, and specific antibodies for detection of endogenous Bcl-2, Bcl-xL or Bax. The ratio of GST-VRK2/actin ranges between 0.72–0.66 in the three bots. The ration of Bcl-xL/actin is 1.50, and the ratio Bax/actin is 1.40, respectively.**(d)** Mapping the interaction between VRK2A and Bcl-xL. The region of interaction between VRK2A and Bcl-xL was performed by pull-down assays with different constructs of the VRK2A protein, which is summarized in a diagram to the right. VRK2B is a spliced variant that has 397 amino acids and is identical to the N-terminal region of VRK2A

To determine if the effect on Bax protein levels was a consequence of an effect mediated by regulation of *BAX* gene expression, the level of *BAX* mRNA was determined by

qt-RT-PCR. Loss of VRK2 using two different siRNAs resulted in a significant increase in the expression of *BAX* mRNA (Figure 3b). Therefore, this result indicated that VRK2

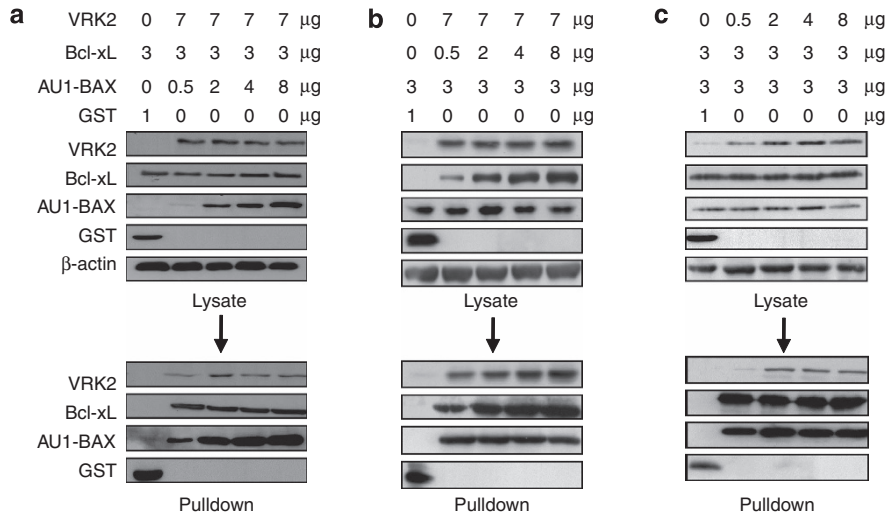


Figure 2 Formation of a complex between VRK2A, Bcl-xL and Bax detected in pull-down assays. (a) Effect of increasing Bax in the presence of saturating amounts of VRK2A and Bcl-xL. (b) Effect of increasing Bcl-xL in the presence of saturating VRK2A and Bax. (c) Effect of increasing VRK2A in the presence of saturating Bcl-xL and Bax. HEK293T cells were transfected with the indicated amounts of plasmids pCEFL-GST-VRK2A, p8-AU1-Bax and p8-Bcl-xL. As a negative control, pCEFL-GST was used. Forty-eight hours after transfection, a GST pull-down was performed. The proteins in the input lysates are shown at the top. The proteins present in the pull-down are shown at the bottom and were detected with the corresponding specific antibody

inhibited *BAX* gene expression. *BCL2* and *Bcl-xl* mRNA levels were also analysed, but no differences in gene expression were detected after VRK2 knockdown (not shown).

Next, it was tested if the effect of VRK2 was mediated by regulation of the *BAX* gene promoter. VRK2 was knocked down in A549 cells with two different siVRK2 oligonucleotides followed by transfection with a proximal *BAX* promoter-luciferase construct, pGL-3-Bax-Luc (−687 to −318), and the effect on luciferase expression was determined. VRK2 knockdown with two different siVRK2, −06 and −08, resulted in six- and eight-fold induction of luciferase expression controlled by the proximal *BAX* gene promoter respectively (Figure 3c). These results indicated that VRK2 protein negatively regulated *BAX* gene expression. Next, as *BAX* gene expression can be activated by treatment with camptothecin,³² it was tested if overexpression of VRK2A was able to prevent this activation of Bax. For this aim, the *BAX* promoter was activated by treating A549 cells with 5 μM camptothecin, and a significant inhibition of the *Bax* promoter was observed in cells in which VRK2A was overexpressed (Figure 3d), but *Bax* promoter was not affected by VRK1 (Figure 3d). All these data indicated that VRK2A inhibited transcription directed by the *BAX* gene promoter.

Loss of VRK2A induced a release of cytochrome c and PARP processing. A subpopulation of the cytosolic VRK2A protein is located in the mitochondria,²⁴ a central organelle in the intrinsic apoptotic pathway. First, the effectiveness of VRK2 knockdown was determined in two lung cancer cell lines, H1299 (p53^{−/−}) and A549 (p53^{+/+}), and in HeLa cells. VRK2A knockdown at protein level was achieved in the three cell lines with two different siRNA, si-VRK2-06 (Figure 4a) and si-VRK2-M (Supplementary Figure S2). In cell culture, these effects of siVRK2 were manifested as a reduction in cell number (not shown), which could be due to the induction of cell death.

To establish if indeed the loss of VRK2A was having an effect on the intrinsic apoptotic pathway, the release of mitochondrial cytochrome *c* and its redistribution in cytosolic and membrane fractions was determined, which is a likely consequence of the effect of VRK2A on Bax. VRK2A knockdown with siVRK2-06 resulted in a significant increase of cytochrome *c* released into the soluble cytosolic fraction, accompanied by a reduction in its mitochondrial level (Figure 4b, top gel). A similar result was also observed using a different siRNA (siVRK2-M) (Supplementary Figure S2). The release of cytochrome *c* should activate caspases that could be detected by processing of PARP. VRK2 knockdown resulted in an increase in the detection of the 85-kDa PARP processed by caspase 9 (Figure 4c). These results indicated that loss of VRK2A facilitated induction of the intrinsic apoptotic pathway and we concluded that high levels of VRK2A have a protective role as inhibitors of apoptosis.

Loss of VRK2 sensitized cells to treatment with camptothecin. The increase in apoptosis as a consequence of reduced levels of VRK2 suggested that cells might become more sensitive to chemotherapy. Therefore, it was studied if elimination of VRK2 made cells more responsive to apoptosis induced by camptothecin, a current drug used in chemotherapy whose mechanism is based on induction of DNA damage. Initiation of apoptosis requires the translocation of Bax to the mitochondrial membrane and release of cytochrome *c*. The distribution of cytochrome *c* and pro-apoptotic Bax was determined by fractionation of cytosolic and membrane fractions. VRK2 was knocked down in HeLa cells and these cells were treated with camptothecin. In cells in which VRK2 was knocked down, there was an increase in cytosolic cytochrome *c*. Membrane-bound Bax appeared much earlier in siVRK2-knocked down cells than si-control-treated cells and at 3 hours, the differences were clearly detectable. (Figure 5a). After 6 hours of camptothecin

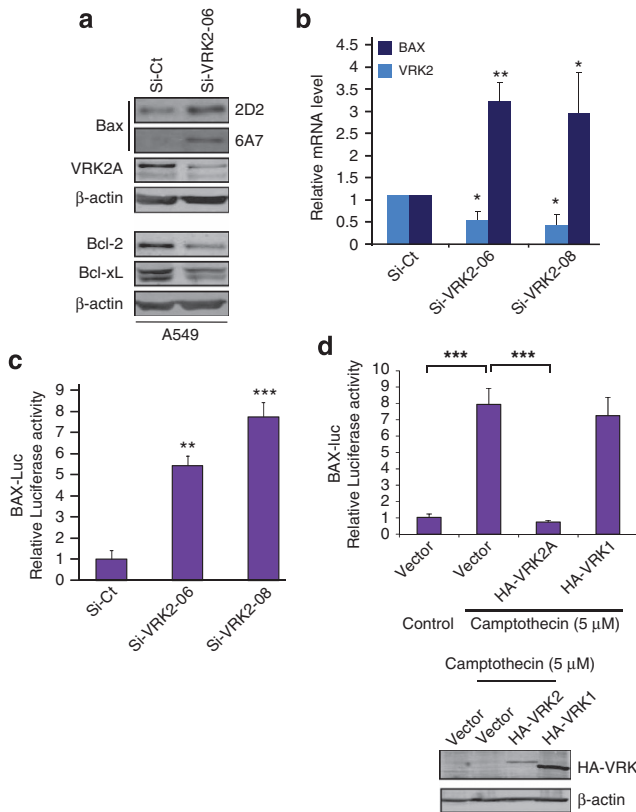


Figure 3 VRK2 regulated BAX expression. (a) VRK2 knockdown in A549 cells modified Bax protein levels. Si-Ct: Si-Control. The total Bax protein was detected with the 2D2 antibody, and activated Bax with 6A7 antibody. Moreover, a reduction in the levels of antiapoptotic proteins, Bcl-xL and Bcl-2 was detected in immunoblots. (b) VRK2 knockdown increased the level of BAX gene expression in A549 cells determined by qt-RT-PCR. A549 cells were mock transfected or transfected with the indicated SiRNA and 3 days after transfection, total RNA was extracted and the level of Bax and GAPDH mRNA levels were determined by qt-RT-PCR. The results from four independent experiments are shown. * $P < 0.05$, ** $P < 0.005$, *** $P < 0.0005$. (c) Reduction of VRK2A levels activated expression from the promoter of BAX. A549 cells were transfected with si-Control (Si-Ct) or two different si-VRK2 (06 and 08, and 24 hours later, cells were transfected with 1 μ g of pGL3-Bax-Luc (-687 to -318) and cells extracts were used to measure the luciferase activity. The results are the mean of three independent experiments and the mean with the standard deviation is shown. ** $P < 0.005$, *** $P < 0.0005$. (d) VRK2A overexpression inhibited expression directed by the BAX gene promoter that is induced in response to camptothecin. A549 cells were treated for 6 hours with 5 μ M camptothecin followed by transfection with 1 μ g of empty vector (pCEFL-HA) or plasmid expressing VRK2A (pCEFL-HA-VRK2A) or VRK1 (pCEFL-HA-VRK1) together with the reporter pGL3-Bax-Luc. The mean and S.D. from three independent experiments is shown. *** $P < 0.0005$

treatment, there was no cytochrome *c* in the membrane fraction and there was an increase in mitochondrial Bax in the membrane fraction in those cells in which VRK2 was knocked down with respect to the control (Figure 5a). This observation suggested that loss of VRK2 facilitates Bax translocation to mitochondria and subsequent release of cytochrome *c*, accelerating induction of apoptosis induced by camptothecin.

This result indicated that loss of VRK2 could be promoting induction of cell death by camptothecin. To further establish that reduced VRK2 levels were inducing apoptosis, the effect of siControl or two different si-VRK2 in cells treated with

camptothecin was detected by determination of PARP processing. VRK2 knockdown by si-VRK2-06 (Figure 5b, top panel) or si-VRK2-M (Figure 5b, bottom panel) made cells more sensitive to induction of apoptosis as shown by the loss of the 116-kDa PARP, which is fully processed at 6 hours of camptothecin treatment (Figure 5b), and was accompanied by the appearance of the 85-kDa processed form of PARP. PARP is a protein implicated in DNA repair, and its inactivation should be reflected by an increase in cellular DNA damage. The effect of VRK2 knockdown on the response to camptothecin was analysed in a tunnel assay. Cells with low levels of VRK2 were positive to DNA damage in the tunnel assay much earlier than siControl cells (Figure 5c).

Loss of VRK2 promoted cell death. All these results indicated that cells were more sensitive to the induction of cell death if VRK2 levels were low. To confirm this possibility, it was first tested if there were early signs of apoptosis in A549 cells in which VRK2 was knocked down. In these cells, there was a very noticeable increase in annexin V + cell positivity at 6 hours of camptothecin treatment, suggesting that the plasma membrane was already altered (Figure 6a), which was also manifested by the increase in nonviable cells detected by uptake of trypan blue (Figure 6b). The alteration of the mitochondrial electron transport and membrane potential as a consequence of initiation of apoptosis could be detected by the uptake and fluorescence of DiOC6 (3). The VRK2 knockdown resulted in a reduction in DiOC6 fluorescence after camptothecin treatment (Figure 6c). Moreover, A549 cells in which VRK2A was knocked down were much more sensitive to DNA fractionation induced by camptothecin treatment, and detected by propidium iodide staining (Figure 6d). Similar results were obtained in H1299 cells and by treatment with other drugs, such as doxorubicin or etoposide (not shown). These results led to the conclusion that reduction of VRK2 levels results in an increased sensitivity to cell death induced by chemotherapeutic drugs.

Discussion

Apoptosis is a tightly regulated process in which many of the components that modulate this form of cell death are still unknown. Regulation of apoptosis can be achieved by multiple mechanisms, but there are likely two major types. One is by novel proteins that form a complex with apoptotic or antiapoptotic proteins, modulating their function. The other is by regulating the expression of apoptotic or anti-apoptotic genes and altering their intracellular levels. In the intrinsic apoptotic pathway, there is an alteration in mitochondrial membrane, and it is likely that other mitochondrial membrane protein complexes remain to be identified, but they can modulate the magnitude of the apoptotic response, and VRK2 could be one of them.

The protective effect observed on apoptosis is partly a consequence of VRK2A interaction with Bcl-xL, which is functionally similar to its interaction with the EBV viral homologue of Bcl-2 and BHRF1.⁸ Both proteins, Bcl-xL and BHRF1, interact with the same C-terminal region of VRK2A.⁸ However, these interactions do not rule out an effect of phosphorylation mediated by VRK2A, particularly if

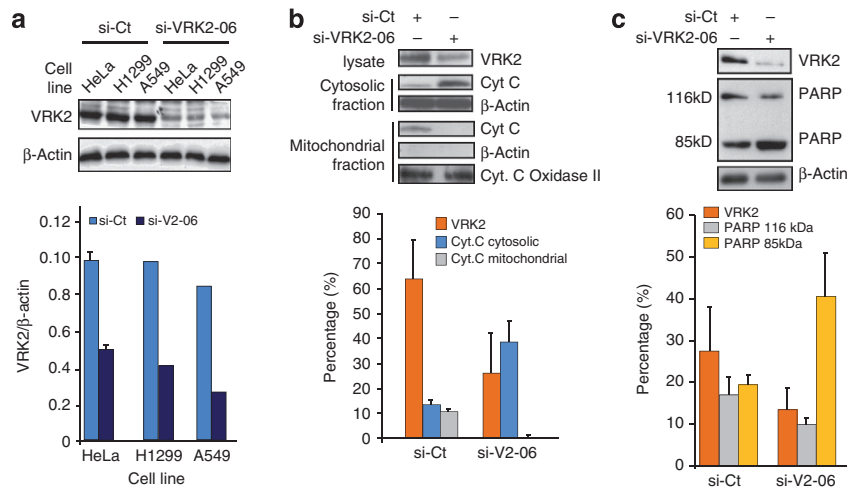


Figure 4 Low levels of VRK2 facilitated release of cytochrome *c* and PARP processing. (a) VRK2 knockdown with si-VRK2-06 and si-Control (si-Ct) in three cell lines, lung carcinomas A549 and H1299 and cervical carcinoma HeLa. The reduction in endogenous protein level and its quantification 4 days after transfection are shown. Endogenous VRK2 protein was detected with a rabbit polyclonal antibody. (b) The release of cytochrome *c* was determined by its detection in cytosolic and mitochondrial fractions in extracts from HeLa cells prepared 96 h after siRNA transfection. The effect of si-VRK2-06 is shown in the top gel panel and quantification of cytochrome *c* distribution in the two fractions, represented as percentage of band intensity respect to the corresponding marker, is shown at the bottom. Actin and cytochrome *c* oxidase II were used as markers for the cytosolic and mitochondrial fractions respectively. (c) Effect of VRK2 knockdown on processing of PARP, a caspase target, in HeLa cells. The proteolytic processing of PARP was determined in a western blot and quantification of the 115 and 85-kDa bands, represented as percentage of band intensity, is shown at the bottom. Immunoblots show a representative experiment and quantifications show the mean and S.D. from three independent experiments

phosphorylations take place as a part of a larger protein complex, which may include Bax among other components. As phosphorylation events are known to modulate apoptosis, phosphorylation of Bax in Ser184, probably by Akt, inhibits effects of Bax in mitochondria and prevents the induction of apoptosis.³³ The VRK2 knockdown does not affect the Akt activation.²⁹ Bax is also phosphorylated by JNK in Ser167, and this phosphorylation is necessary for Bax activation and translocation to mitochondria.³⁴ VRK2A does not phosphorylate Bax, but it is possible that VRK2A in the mitochondrial membrane complex might phosphorylate some protein not yet identified. This might either interfere with Bax incorporation or alternatively alter mitochondrial membranes, facilitating its permeability and cytochrome *c* release.

Variations in intracellular VRK2A protein levels, either by knockdown or overexpression, also affect the levels of Bax. This effect is mediated by the regulation of the *BAX* promoter by VRK2A, functioning as a negative regulator of this promoter. The VRK2A function as a transcriptional repressor opens up a new aspect in the role of VRK2 as a regulator of transcription. Thus, VRK2A is acting at two different levels in the modulation of the cell response to induction of apoptosis: protein–protein interaction and transcriptional regulation.

The effects of VRK2A observed on cell signalling can also be influenced by the consequences of other VRK2A protein interactions. VRK2A interacts with scaffold proteins and inhibits signal transmission. VRK2A interacts with JIP1, a JNK scaffold, blocking *c*-Jun phosphorylation.^{27,28} VRK2A also interacts with KSR1 blocking the phosphorylation of ERK, but has no effect on Akt activation, facilitating cell survival.²⁹

Most of the effects identified by VRK2 are mediated by protein–protein interaction and theoretically will require the design of drugs targeting the specific interaction. However, inhibition of VRK2 activity with kinase inhibitors will affect

signal transduction by a not yet known pathway. The first role of VRK2 as an active kinase phosphorylating NFAT1 has been recently reported,³⁵ although VRK2 phosphorylates some scaffold proteins like JIP-1 (Jun interacting protein 1) that mediate signals in response to cytokines, such as IL-1 β ²⁸ or hypoxia,²⁷ but the effect of VRK2 on JIP1 is only dependent of protein interaction. The field of protein interactions inhibitors is not developed; although it will permit selective inhibition of some effects, but not other effects mediated by a specific protein. In the case of VRK2, induction of its interaction with Bcl-xL will result in an increase of the protective effect of Bcl-xL. The structures of VRK2¹⁴ and VRK1³⁶ indicate that both kinases have a characteristic catalytic domain that differs from most kinases in several key residues,^{10,13} but nevertheless, it is still catalytically active.^{12,13,24} These differences in VRK proteins can be exploited for the development of specific kinase inhibitors. VRK proteins are likely to have a very low promiscuity,³⁷ and this is an advantage with respect to other kinases where the problem of cross inhibition is very high.^{38,39} VRK2 has a very low promiscuity index with respect to kinase inhibitors,^{37,40} and is very insensitive to current kinase inhibitors.⁴¹ The development of VRK2-specific inhibitors might be a potential mechanism to increase cell sensitivity to current drugs, which are very toxic.

The effect of VRK2 knockdown on cellular sensitivity to apoptosis induced by DNA-damaging drugs is unlikely to be specific. VRK2 knockdown probably sensitizes cells to any type of stress by reducing the effectiveness of Bcl-xL on apoptosis protection and thus permitting increased levels and liberation of Bax. In breast carcinoma, there is an inverse correlation between the levels of ERBB2 and VRK2, thus, ERBB2-positive tumours have low VRK2 and curiously, these tumours are more chemosensitive.²⁹ Breast cancers that are

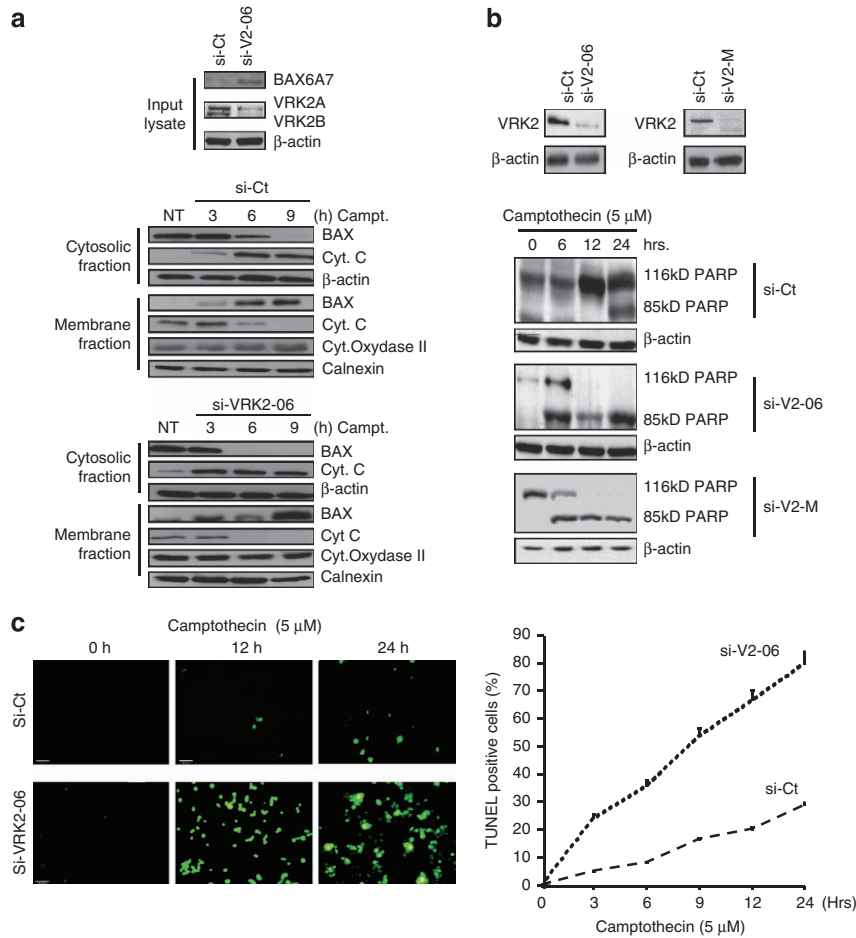


Figure 5 Low levels of VRK2 sensitized cells to camptothecin treatment. (a) VRK2 knockdown was induced in A549 cells. These cells were treated with 5 μ M of camptothecin and the distribution of cytochrome *c* and Bax were determined in cytosolic and membrane fractions at different time points after camptothecin addition. Fractionated extracts were used for western blot analysis with the corresponding antibodies. (b) Low VRK2 facilitated activation of caspases in response to treatment with 5 μ M camptothecin. VRK2 knockdown was induced by two different siRNA, si-VRK2-06 (at the top) or si-VRK2-2M (at the bottom), and caspase activation was determined by PARP processing. PARP was determined by immunoblot with a specific antibody at different time points after camptothecin addition to A549 cell culture. (c) Loss of VRK2 facilitated induction of DNA damage by camptothecin. A549 cells were transfected with si-Control or si-VRK2-06 and 96 hours later, they were treated with 5 μ M of camptothecin. A TUNEL assay was performed to detect the presence of free DNA ends at different time points. Cells labelled with fluorescein-12-dTUP (rTdT) and propidium iodide were analysed in a fluorescence microscope. Cell images with fluorescence are shown in the left panel and in the right panel the quantification of TUNEL positive cells are shown as a function of time following treatment with camptothecin. Si-Ct: si-control. siV2: si-VRK2-06

ERBB2-negative and oestrogen receptor-positive have high levels of VRK2,²⁹ and these tumours are chemoresistant,^{42,43} probably by induction of p53- and p21-mediated cell cycle arrest.⁴⁴

In tumours, high VRK2 levels can have a dual role, on one side, they might inhibit mitogenic signal-reducing tumour growth, but on the other hand, they might make cells less sensitive to apoptosis, contributing to tumour cell survival. The final effect would be a consequence of the net balance among alternative signalling pathways and the relative strength of their respective signals. Thus, high VRK2 levels might be a component in the formation of more indolent and perhaps, chemoresistant tumours.

Materials and Methods

Cell culture and flow cytometry. Cell lines A549 (p53 wt) and H1299 (p53 -/-) from lung carcinomas, HEK293T cells and HeLa cells were cultured at 37 °C with 5% CO₂ in RPMI or DMEM supplemented with 10% heat-inactivated foetal calf serum supplemented with 2 mM L-glutamine, 50 μ g/ml streptomycin and

100 U/ml penicillin. All cell lines were purchased from ATCC. For flow cytometry analysis, cells were fixed with 4% paraformaldehyde and incubated with propidium iodide. Cells were analysed in a FACScalibur flow cytometer, (Becton Dickinson, San Jose, CA, USA), data acquisition was performed with Cell Quest programme (Becton Dickinson), analysed with Modfit LT programme (Verity Software House, Topsham, ME, USA).

Preparation of cytosolic and membrane subcellular fractions.

Cells were washed twice in cold PBS at 4 °C and 2300 r.p.m in an Eppendorf 5415R centrifuge. The cellular pellet was lysed in a buffer containing 25 mM TrisHCl (pH 6.8), 250 mM sucrose, 1 mM EDTA, 0.1 mM benzamidine and 1 μ g/ml each of leupeptin, pepstatin and aprotinin. The suspension was centrifuged at 13000 r.p.m in an Eppendorf 5415R centrifuge for 3 min. The supernatant was centrifuged at 100000 \times g for 1 h at 4 °C and the pellet contained the endoplasmic reticulum and mitochondrial membranes.²¹

Chemicals. Camptothecin and propidium iodide were from Sigma (St. Louis, MO, USA). DiOC₆(3) (3,3'-Dihexyloxacarbocyanine iodide) was from Molecular Probes (Eugene, OR, USA). Annexin V-FITC was from Immunostep (Salamanca, Spain).

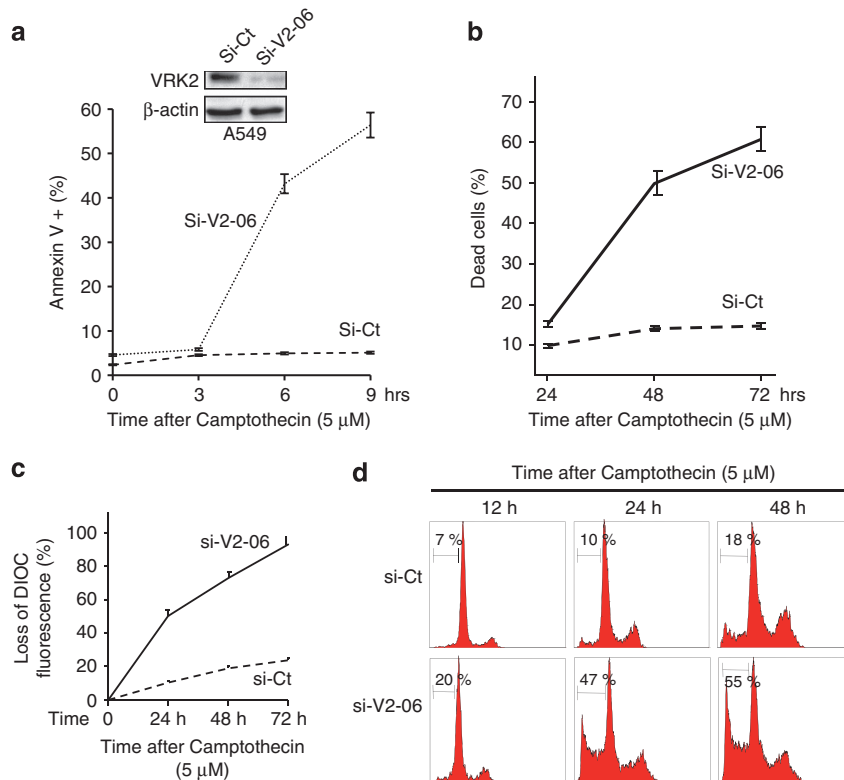


Figure 6 Effect of VRK2 knockdown on cell death induced by camptothecin treatment. VRK2 was knocked down in A549 cells and after 3 days, cells were treated with camptothecin for the indicated time points. (a) Effect of VRK2 knockdown on the sensitivity of A549 cells to camptothecin detected by alterations in the plasma membrane with annexin V + . Cells were stained with AnnexinV-FITC and positive cells were counted by flow cytometry. (b) Effect of VRK2 knockdown on A549 cell viability after camptothecin treatment. Viability was determined by Trypan blue dye exclusion assay. (c) Effect of VRK2 knockdown on mitochondrial membrane potential in the response to camptothecin was determined by loss of DiOC6 fluorescence in damaged cells. (d). Effect of camptothecin (5 μM) on A549 cells and detection of propidium iodide staining by flow cytometry. The fragmented DNA was detected in the sub-G0/G1 window (bar). Si-Ct: si-control. siV2-06: si-VRK2-06

Plasmids and transfections. VRK2 was expressed from plasmid pCEFL-GST-VRK2A, pCEFL-HA-VRK2A, pCEFL-GST-VRK2B and deletion or partial constructs with regions 1–320, 256–508, 364–508 and 256–397.^{24,27,28} pCMV-FLAG-PUMA α was from K Vousden,⁴⁵ Bax and Bcl-xL were expressed from plasmids p8-AU1-Bax and p8-Bcl-xL (from F Pimentel).⁴⁶ Bad from PCDNA3-AU1-BAD (L del Peso). Bcl-2 from pSFFV-Bcl2 (JL Fernández-Luna). Empty vector plasmids, pCEFL-GST and pCEFL-HA, were used as negative controls in transfections.²⁴ pGL-3-Bax-Luc (– 687 to – 318) was from M Oren (Weitzman Institute, Rehovot, Israel).⁴⁷ Luciferase assays have been previously reported.^{24,48} Transfections were performed using JetPEI reagent (Polyplus, Illkirch, France) according to manufacturer's instructions and in detail has been previously published.^{24,28,29,35,49} The total amount of DNA was kept constant by completion with the corresponding empty vector.

RNA and qt-RT-PCR. Total RNA was extracted from A549 cells using RNeasy kit from Qiagen (Valencia, CA, USA). The quality of the extracted RNA was determined in a Bioanalyzer 2100 nano-lab chip (Agilent, Santa Clara, CA, USA). For qtRT-PCR, 50 μg of total RNA was amplified with specific primers for Bax, VRK2 and GAPDH. The Quantitect-SYBR green RT-PCR kit (Qiagen) was used in an iCycler iQ5 Multicolour Real-time PCR Detection System and Optical System Software BIO-RAD iQ5 (BioRad, Hercules, CA, USA).

The following primers were used for RT-PCR amplification. The following primers were used for RT-PCR amplification. Bax was amplified with primers (forward: 5'-GGCCACCAGCTCTGAGCAGA-3', and reverse: 5'-GCCACGTGGGCGTCCCAAAGT-3'). Bcl-xL (forward: 5'-TCCTGTGCTACGCTTTCCACG-3'; reverse: 5'-GGTCCGATTGTGGCCTTT-3'). Bcl-2 (forward: 5'-CATGTGTGTGGAGAGCGTCAA-3' and reverse: 5'-GCCGGTTCAGGTACTCAGTCA-3'). VRK2 (forward: 5'-AGTGAGAGAAGCGCTGAGTCT-3' and reverse: 5'-CAAAGTCTTGTGAGACTCTTG-3'). GAPDH (forward: 5'-GGTCTACTCCTTGAGGCCATGTG-3' and

reverse: 5'-ACCTAACTACATGGTTTACATGTT-3'). All primers were synthesized by Sigma-Aldrich (St Louis, MO, USA).

VRK2 knockdown. VRK2 knockdown was performed with three different siRNA. Si-VRK2-06 (target sequence: GCAAGGUUCUGGAUGAUU) and siVRK2-08 (target sequence: CACAAUAGGUUAAUCGAAA) from Dharmacon (Chicago, IL, USA), and si-VRK2-M (target sequence: GATATTGTCCCAATGGGAA) from Mission series (Sigma, St Louis, MO, USA). Si-Control was from Dharmacon. 160 nM of si-Control or si-VRK2 was lipofectamine 2000 (Invitrogen, Carlsbad, CA, USA) according to manufacturer's instructions. These type of RNA interference have been previously performed and described in detail for VRK2.^{24,28,29,35,49}

Antibodies. VRK2 was detected with a rabbit polyclonal antibody^{24,28,29,49} that recognized both isoforms and was prepared by immunization of a rabbit with human GST-VRK2A fusion protein. AU1 epitope was detected with monoclonal or polyclonal antibodies from Covance (Emeryville, CA, USA). GST was detected with monoclonal B-14 (sc-138, Santa Cruz Biotechnology, Santa Cruz, CA, USA). HA epitope was detected with monoclonal (Covance) or polyclonal antibody (eBioscience, San Diego, CA, USA). Flag was detected with polyclonal and monoclonal antibodies from Sigma. Monoclonal antibodies against Bax (6A7), Bcl-xL (2H12), cytochrome *c* (7H8.2C12) and PARP (c2-10) were from BD Biosciences (San Jose, CA, USA). Cleaved PARP was detected with monoclonal antibody (F21-852) from BD Biosciences. Rabbit polyclonal anti-Bax was from Abcam (Cambridge, UK). Bcl-2 was detected with sc-492 from Santa Cruz. Cytochrome oxidase II was detected with a monoclonal from Invitrogen. β -actin antibody was from Sigma. The secondary antibodies used from Amersham Biosciences (GE Healthcare, Buckinghamshire, UK) were anti-mouse-Cy2 (Fluorolink Cy2), anti-rabbit-Cy3 (Fluorolink Cy3) and anti-rabbit-Cy2 (Fluorolink Cy2) in immunofluorescence or anti-mouse-HRP or anti-rabbit-HRP for western blots.

Pulldown assays and immunoblotting. Cells were harvested 48 h post transfection and lysed with a buffer containing 20 mM Tris-HCl pH 7.4, 137 mM NaCl, 2 mM EDTA, 25 mM β -glycerophosphate, 2 mM pyrophosphate, 10% (v/v) glycerol and 1% Triton X-100 plus protease inhibitors. 50 μ g of total protein lysate were analysed in a 10% SDS-polyacrylamide gel. GST pulldowns were performed by incubating 1 mg of total cell extract with Glutathione-Sepharose 4B beads (Amersham Biosciences Pharmacia Biotech) for 12 h at 4 °C. Sepharose beads were washed three times with lysis buffer and analysed by SDS-PAGE following by western blots with the corresponding antibodies. Luminescence in western blot was developed with an ECL kit (Amersham Biosciences).

Early apoptosis and annexin V assay. Early apoptotic cells present phosphatidylserine on their surface and were detected by flow cytometry of cells labelled with Annexin V-FITC (Immunostep SL, Salamanca, Spain). HeLa, A549 and H1299 cells were grown and transfected with siControl or siVRK2 as indicated above and 96 hours later, treated with camptothecin (5 μ M). At different time points, 10⁶ cells were washed in PBS and stained with annexin-V-FITC and propidium iodide in annexin buffer (0.1 M HEPES/NaOH (pH 7.4) 1.4 M NaCl, 25 mM CaCl₂), incubated for 15 min, resuspended in 400 μ l and analysed by flow cytometry in a FACS Calibur (Becton Dickinson).

Immunofluorescence and TUNEL assay. Colocalization of proteins was performed by immunofluorescence. Cells were fixed with 3% paraformaldehyde and stained with specific antibodies against endogenous proteins. Nuclei were stained with DAPI (4',6'-diamidino-2-fenilindol). Immunofluorescences were examined in a confocal Zeiss LSM 510 microscope (Zeiss, Jena, Germany) and images were analysed with LSM Image Browser software (Zeiss).

To perform TUNEL assay, the cells were transfected with siRNA and treated with camptothecin (5 μ M). At different time points, the culture media was removed and cells were fixed with 4% paraformaldehyde for 15 min, washed with cold PBS and treated with 0.2% Triton-X100 for 5 min. Cells were blocked for 15 min in incubation buffer (200 mM potassium cacodylate, 25 mM Tris-HCl, 0.2 mM DTT, 0.25 mg/ml BSA, 2.5 mM cobalt hydrochloride) at room temperature. The buffer was changed and 5 μ l per point were added containing 50 μ M fluorescein-12-dUTP, 100 μ M dATP, 10 mM Tris-HCl (pH 7.6), 1 mM EDTA for rTdT. Cells were incubated in a humidified atmosphere in the dark for 1 h at 37 °C. The reaction was finished by addition of 1 ml 20 \times SSC for 15 min and afterwards cells were rinsed in PBS three times. The coverslips were treated with antifade and examined in a confocal Zeiss Axioplan2 microscope. Images were analysed using the Openlab 4.0.2 program (Improvision, Waltham, MA, USA).

Mitochondrial membrane potential determination. To determine membrane permeabilisation ($\Delta\Psi_m$) DiOC6³ (yodo 3-3'-dihexiloxacarbocianine) was used.^{50,51} For this assay, 2 \times 10⁶ A549 cells/ml were seeded in six-well plates. Cells were transfected with si-Control, siVRK2-06, or siVRK2-M, as previously reported.^{21,52} Ninety-six hours later, cells were treated with 5 μ M and collected for analysis at several time points up to 72 h after drug treatment. These cells were washed in PBS and collected by centrifugation at 15 000 r.p.m for 10 min. The cell pellet was suspended in PBS containing 20 nM DiOC6 and was incubated at 26 °C for 20 min. Cells were analysed in a FACS-Calibur (Becton Dickinson) with the Cell Quest and FCS Express V3 programs (De novo software, Los Angeles, CA, USA).

Conflict of Interest

The authors declare no conflict of interest.

Acknowledgements. DMM, IFF and MV-C, have JAE-CSIC-Fondo Social Europeo Predoctoral fellowships. TM and SB were funded by CSIC-Banco Santander and Ministerio de Ciencia e Innovación fellowships respectively. This work was funded by grants from Ministerio de Ciencia e Innovación (SAF2010-14935 and CSD2007-0017), and Kutxa-Fundación Inbiomed.

1. Tsumimoto Y, Cossman J, Jaffe E, Croce CM. Involvement of the bcl-2 gene in human follicular lymphoma. *Science* 1985; **228**: 1440–1443.
2. Reed JC. Proapoptotic multidomain Bcl-2/Bax-family proteins: mechanisms, physiological roles, and therapeutic opportunities. *Cell Death Differ* 2006; **13**: 1378–1386.

3. Youle RJ, Strasser A. The BCL-2 protein family: opposing activities that mediate cell death. *Nat Rev Mol Cell Biol* 2008; **9**: 47–59.
4. Taylor RC, Cullen SP, Martin SJ. Apoptosis: controlled demolition at the cellular level. *Nat Rev Mol Cell Biol* 2008; **9**: 231–241.
5. Levine B, Sinha S, Kroemer G. Bcl-2 family members: dual regulators of apoptosis and autophagy. *Autophagy* 2008; **4**: 600–606.
6. Martinou JC, Youle RJ. Mitochondria in apoptosis: bcl-2 family members and mitochondrial dynamics. *Dev Cell* 2011; **21**: 92–101.
7. Ow YL, Green DR, Hao Z, Mak TW. Cytochrome c: functions beyond respiration. *Nat Rev Mol Cell Biol* 2008; **9**: 532–542.
8. Li LY, Liu MY, Shih HM, Tsai CH, Chen JY. Human cellular protein VRK2 interacts specifically with Epstein-Barr virus BHRF1, a homologue of Bcl-2, and enhances cell survival. *J Gen Virol* 2006; **87**: 2869–2878.
9. Nichols RJ, Wiebe MS, Traktman P. The vaccinia-related kinases phosphorylate the N' terminus of BAF, regulating its interaction with DNA and its retention in the nucleus. *Mol Biol Cell* 2006; **17**: 2451–2464.
10. Manning G, Whyte DB, Martinez R, Hunter T, Sudarsanam S. The protein kinase complement of the human genome. *Science* 2002; **298**: 1912–1934.
11. Klerx EP, Lazo PA, Askjaer P. Emerging biological functions of the vaccinia-related kinase (VRK) family. *Histol. Histopathol* 2009; **24**: 749–759.
12. Lopez-Borges S, Lazo PA. The human vaccinia-related kinase 1 (VRK1) phosphorylates threonine-18 within the mdm-2 binding site of the p53 tumour suppressor protein. *Oncogene* 2000; **19**: 3656–3664.
13. Nichols RJ, Traktman P. Characterization of three paralogous members of the Mammalian vaccinia related kinase family. *J Biol Chem* 2004; **279**: 7934–7946.
14. Scheeff ED, Eswaran J, Bunkoczi G, Knapp S, Manning G. Structure of the pseudokinase VRK3 reveals a degraded catalytic site, a highly conserved kinase fold, and a putative regulatory binding site. *Structure* 2009; **17**: 128–138.
15. Sanz-Garcia M, Lopez-Sanchez I, Lazo PA. Proteomics identification of nuclear Ran GTPase as an inhibitor of human VRK1 and VRK2 (vaccinia-related kinase) activities. *Mol Cell Proteomics* 2008; **7**: 2199–2214.
16. Kim W, Chakraborty G, Kim S, Shin J, Park CH, Jeong MW et al. Macro Histone H2A1.2 (MacroH2A1) Protein Suppresses Mitotic Kinase VRK1 during Interphase. *J Biol Chem* 2012; **287**: 5278–5289.
17. Valbuena A, Sanz-Garcia M, Lopez-Sanchez I, Vega FM, Lazo PA. Roles of VRK1 as a new player in the control of biological processes required for cell division. *Cell Signal* 2011; **23**: 1267–1272.
18. Valbuena A, Lopez-Sanchez I, Lazo PA. Human VRK1 is an early response gene and its loss causes a block in cell cycle progression. *PLoS ONE* 2008; **3**: e1642.
19. Kang TH, Park DY, Kim W, Kim KT. VRK1 phosphorylates CREB and mediates CCND1 expression. *J Cell Sci* 2008; **121**: 3035–3041.
20. Sanz-Garcia M, Monsalve DM, Sevilla A, Lazo PA. Vaccinia-related Kinase 1 (VRK1) is an upstream nucleosomal kinase required for the assembly of 53BP1 foci in response to ionizing radiation-induced DNA damage. *J Biol Chem* 2012; **287**: 23757–23768.
21. Lopez-Sanchez I, Sanz-Garcia M, Lazo PA. Plk3 interacts with and specifically phosphorylates VRK1 in Ser342, a downstream target in a pathway that induces Golgi fragmentation. *Mol Cell Biol* 2009; **29**: 1189–1201.
22. Sevilla A, Santos CR, Barcia R, Vega FM, Lazo PA. c-Jun phosphorylation by the human vaccinia-related kinase 1 (VRK1) and its cooperation with the N-terminal kinase of c-Jun (JNK). *Oncogene* 2004; **23**: 8950–8958.
23. Sevilla A, Santos CR, Vega FM, Lazo PA. Human vaccinia-related kinase 1 (VRK1) activates the ATF2 transcriptional activity by novel phosphorylation on Thr-73 and Ser-62 and cooperates with JNK. *J Biol Chem* 2004; **279**: 27458–27465.
24. Blanco S, Klimcakova L, Vega FM, Lazo PA. The subcellular localization of vaccinia-related kinase-2 (VRK2) isoforms determines their different effect on p53 stability in tumour cell lines. *FEBS J* 2006; **273**: 2487–2504.
25. Sanz-Garcia M, Vazquez-Cedeira M, Kellerman E, Renbaum P, Levy-Lahad E, Lazo PA. Substrate profiling of human vaccinia-related kinases identifies coilin, a Cajal body nuclear protein, as a phosphorylation target with neurological implications. *J Proteomics* 2011; **75**: 548–560.
26. Vázquez-Cedeira M, Barcia-Sanjujo I, Sanz-Garcia M, Barcia R, Lazo PA. Differential inhibitor sensitivity between human kinases VRK1 and VRK2. *PLoS ONE* 2011; **6**: e23235.
27. Blanco S, Santos C, Lazo PA. Vaccinia-related kinase 2 modulates the stress response to hypoxia mediated by TAK1. *Mol Cell Biol* 2007; **27**: 7273–7283.
28. Blanco S, Sanz-Garcia M, Santos CR, Lazo PA. Modulation of interleukin-1 transcriptional response by the interaction between VRK2 and the JIP1 scaffold protein. *PLoS ONE* 2008; **3**: e1660.
29. Fernandez IF, Blanco S, Lozano J, Lazo PA. VRK2 inhibits mitogen-activated protein kinase signaling and inversely correlates with ErbB2 in human breast cancer. *Mol Cell Biol* 2010; **30**: 4687–4697.
30. Fernandez IF, Perez-Rivas LG, Blanco S, Castillo-Dominguez AA, Lozano J, Lazo PA. VRK2 anchors KSR1-MEK1 to endoplasmic reticulum forming a macromolecular complex that compartmentalizes MAPK signaling. *Cell Mol Life Sci* 2012; **64**: 3881–3893.
31. Degterev A, Yuan J. Expansion and evolution of cell death programmes. *Nat Rev Mol Cell Biol* 2008; **9**: 378–390.
32. Lin L, Ozaki T, Takada Y, Kageyama H, Nakamura Y, Hata A et al. topors, a p53 and topoisomerase I-binding RING finger protein, is a coactivator of p53 in growth suppression induced by DNA damage. *Oncogene* 2005; **24**: 3385–3396.

33. Gardai SJ, Hildeman DA, Frankel SK, Whitlock BB, Frasch SC, Borregaard N *et al*. Phosphorylation of Bax Ser184 by Akt regulates its activity and apoptosis in neutrophils. *J Biol Chem* 2004; **279**: 21085–21095.
34. Kim BJ, Ryu SW, Song BJ. JNK- and p38 kinase-mediated phosphorylation of Bax leads to its activation and mitochondrial translocation and to apoptosis of human hepatoma HepG2 cells. *J Biol Chem* 2006; **281**: 21256–21265.
35. Vazquez-Cedeira M, Lazo PA. Human VRK2 (Vaccinia-related Kinase 2) modulates tumor cell invasion by hyperactivation of NFAT1 and expression of cyclooxygenase-2. *J Biol Chem* 2012; **287**: 42739–42750.
36. Shin J, Chakraborty G, Bharatham N, Kang C, Tochio N, Koshiba S *et al*. NMR solution structure of human vaccinia-related kinase 1 (VRK1) reveals the C-terminal tail essential for its structural stability and autocatalytic activity. *J Biol Chem* 2011; **286**: 22131–22138.
37. Fedorov O, Marsden B, Pogacic V, Rellos P, Muller S, Bullock AN *et al*. A systematic interaction map of validated kinase inhibitors with Ser/Thr kinases. *Proc Natl Acad Sci USA* 2007; **104**: 20523–20528.
38. Zhang J, Yang PL, Gray NS. Targeting cancer with small molecule kinase inhibitors. *Nat Rev Cancer* 2009; **9**: 28–39.
39. Knight ZA, Lin H, Shokat KM. Targeting the cancer kinome through polypharmacology. *Nat Rev Cancer* 2010; **10**: 130–137.
40. Fedorov O, Sundstrom M, Marsden B, Knapp S. Insights for the development of specific kinase inhibitors by targeted structural genomics. *Drug Discov Today* 2007; **12**: 365–372.
41. Vazquez-Cedeira M, Barcia-Sanjurjo I, Sanz-Garcia M, Barcia R, Lazo PA. Differential Inhibitor Sensitivity between Human Kinases VRK1 and VRK2. *PLoS ONE* 2011; **6**: e23235.
42. Rouzier R, Perou CM, Symmans WF, Ibrahim N, Cristofanilli M, Anderson K *et al*. Breast cancer molecular subtypes respond differently to preoperative chemotherapy. *Clin. Cancer Res* 2005; **11**: 5678–5685.
43. Rouzier R, Pusztai L, Delaloge S, Gonzalez-Angulo AM, Andre F, Hess KR *et al*. Nomograms to predict pathologic complete response and metastasis-free survival after preoperative chemotherapy for breast cancer. *J Clin Oncol* 2005; **23**: 8331–8339.
44. Deisenroth C, Thorner AR, Enomoto T, Perou CM, Zhang Y. Mitochondrial Hep27 is a c-Myb target gene that inhibits Mdm2 and stabilizes p53. *Mol Cell Biol* 2010; **30**: 3981–3993.
45. Nakano K, Vousden KH. PUMA a novel proapoptotic gene, is induced by p53. *Mol Cell* 2001; **7**: 683–694.
46. Klee M, Pimentel-Muinon FX. Bcl-X(L) specifically activates Bak to induce swelling and restructuring of the endoplasmic reticulum. *J Cell Biol* 2005; **168**: 723–734.
47. Miyashita T, Reed JC. Tumor suppressor p53 is a direct transcriptional activator of the human bax gene. *Cell* 1995; **80**: 293–299.
48. Vega FM, Sevilla A, Lazo PA. p53 stabilization and accumulation induced by human vaccinia-related kinase 1. *Mol Cell Biol* 2004; **24**: 10366–10380.
49. Fernandez IF, Perez-Rivas LG, Blanco S, Castillo-Dominguez AA, Lozano J, Lazo PA. VRK2 anchors KSR1-MEK1 to endoplasmic reticulum forming a macromolecular complex that compartmentalizes MAPK signaling. *Cell Mol Life Sci* 2012; **69**: 3881–3893.
50. Gajate C, Santos-Beneit AM, Macho A, Lazaro M, Hernandez-De Rojas A, Modolell M *et al*. Involvement of mitochondria and caspase-3 in ET-18-OCH(3)-induced apoptosis of human leukemic cells. *Int J Cancer* 2000; **86**: 208–218.
51. Reis-Sobreiro M, Gajate C, Mollinedo F. Involvement of mitochondria and recruitment of Fas/CD95 signaling in lipid rafts in resveratrol-mediated antimyeloma and antileukemia actions. *Oncogene* 2009; **28**: 3221–3234.
52. Valbuena A, Vega FM, Blanco S, Lazo PA. p53 downregulates its activating vaccinia-related kinase 1, forming a new autoregulatory loop. *Mol Cell Biol* 2006; **26**: 4782–4793.



Cell Death and Disease is an open-access journal published by Nature Publishing Group. This work is licensed under the Creative Commons Attribution-NonCommercial-No Derivative Works 3.0 Unported License. To view a copy of this license, visit <http://creativecommons.org/licenses/by-nc-nd/3.0/>

Supplementary Information accompanies this paper on Cell Death and Disease website (<http://www.nature.com/cddis>)